

PALYGORSKITE IN EOCENE-OLIGOCENE LAGOONAL ENVIRONMENT, YUCATÁN, MEXICO

Liberto de Pablo-Galán*

ABSTRACT

Palygorskite occurs in the Yucatán peninsula as palygorskite-rich mudstone in middle Eocene Chichén-Itzá formation to Oligocene. Its lower limit of deposition is the lower Eocene Pisté formation or the Xbacal member of the middle Eocene Chichén-Itzá formation. It is overlain by diagenized Mg-limestone. Palygorskite mud also occurs as lenses in Oligocene calcareous marl, overlain by dolomitic marl. Two clay systems predominate in Yucatán. One, pedogenic, corresponds to the more mature soils of the northern platform and is characterized by b-axis disordered kaolinite associated with minor calcite and quartz. The second system is typified by palygorskite associated with minor illite/smectite, smectite, opal, calcite, chert, and gypsum. Palygorskite formed in a tranquil marine back-reef lagoon environment of high Mg, Si, and Al activities, by diagenesis of precursor montmorillonite, from reaction between montmorillonite, dolomitic limestone, and silicic acid from the limestone or carried into the basin from external sources, resulting in palygorskite and authigenic calcite.

Key words: Clay geochemistry, palygorskite, Yucatán, Mexico.

RESUMEN

La palygorskita se presenta en la península de Yucatán en una lodolita rica en palygorskita de la formación Chichén-Itzá, que varía en edad del Eoceno medio al Oligoceno. Su límite inferior de depósito es la formación Pisté, del Eoceno inferior, o el miembro Xbacal, del Eoceno medio, de la formación Chichén-Itzá. Se encuentra cubierta por caliza magnesiana diagenética. El lodo con palygorskita también se presenta como lentes en marga calcárea del Oligoceno, cubierta por marga dolomítica. Dos sistemas de arcilla predominan en Yucatán: Uno, pedogénico, corresponde a los suelos más maduros de la plataforma septentrional y está caracterizado por caolinita desordenada de eje b asociada con calcita y cuarzo subordinados. El otro está tipificado por palygorskita asociada con illita/esmectita, esmectita, ópalo, calcita, pedernal y yeso subordinados. La palygorskita se formó en un ambiente marino tranquilo de laguna postarrecifal, con actividades altas de Mg, Si, y Al, por diagénesis de montmorillonita precursora, a través de la reacción entre montmorillonita, caliza dolomítica y ácido silícico de la caliza o transportados a la cuenca de fuentes externas, resultando en palygorskita y calcita autigénica.

Palabras clave: Geoquímica de arcillas, palygorskita, Yucatán, México.

INTRODUCTION

Palygorskite is a clay mineral not common in Mexico. The only known deposits occur in the Yucatán peninsula, where Eocene-Oligocene palygorskite-rich mudstone occurs in the form of lenses and plug-like deposits in sedimentary rocks. The extension and economic significance of these deposits have not been studied, and most of the published literature has been on the genesis of the deposits (Isphording, 1973; de Pablo-Galán, 1971; Bohor, 1975; Arnold and Bohor, 1978), which concedes that palygorskite was formed by direct crystallization from marine waters or during diagenesis of dolomitic limestones.

The origin of palygorskite has been a controversial issue in clay mineralogy. The mineral occurs in marine and lacustrine sediments, in arid and saline environments, or associated with hydrothermal activities (Van den Heuvel, 1966; Patterson, 1974; Singer and Norrish, 1974; Yaalon and Wieder, 1976; Weaver and Beck, 1977; Singer, 1979; Callen, 1984; Estéoule-Choux, 1984; Singer, 1984; Shadfan *et al.*, 1985;

Jones and Galán, 1988). In general, it is accepted that palygorskite may form by dissolution-precipitation processes, by neoformation (Isphording, 1973, 1984; Estéoule-Choux, 1984), transformed from illite (Galán and Castillo, 1984; Sánchez and Galán, 1995) or from smectite (Singer, 1984; Sánchez and Galán, 1995), or by reaction involving montmorillonite, dolomite, and siliceous materials (Tardy and Garrels, 1974; Singer and Norrish, 1974; Weaver and Beck, 1977; Jones, 1986). The present study attempts to contribute to the knowledge on the genesis of palygorskite by describing the palygorskite that occurs in the Yucatán peninsula, suggesting possible processes for its genesis.

GEOGRAPHIC AND GEOLOGIC SETTING

Palygorskite-rich mudstone occurs in the Yucatán peninsula, within an Eocene-Oligocene formation that is located between the 89°00' and 90°25' W and 18°25' to 18°70' N. The geology of the Yucatán peninsula has been presented by several authors (Álvarez, 1954; Butterlin and Bonet, 1960; Bonet and Butterlin, 1962; Weidie and Murray, 1962; West, 1962; López-Ramos, 1979), but it still remains largely unknown due to the absence of surface crops and mineral deposits and to the ubiquitous cover of caliche.

*Instituto de Geología, Universidad Nacional Autónoma de México, Ciudad Universitaria, Delegación Coyoacán, 04510 D.F., Mexico.

The subsurface geology is better known from oil exploration wells. The peninsula became emergent during the Pleistocene. Three physiographic units are differentiated: (1) the Sierra de Ticul or Puuk, which is an upper Paleocene-Eocene fault scarp of dolomitized ferruginous limestone rising 50 to 110 m, 110 km long, that dissects the peninsula in the NW-SE direction; (2) the central lowland, which extends south of the sierra into the Petén peninsula and the Maya mountains of Guatemala; (3) the northern platform, that stretches north of the sierra out to the Gulf of Mexico (Figure 1).

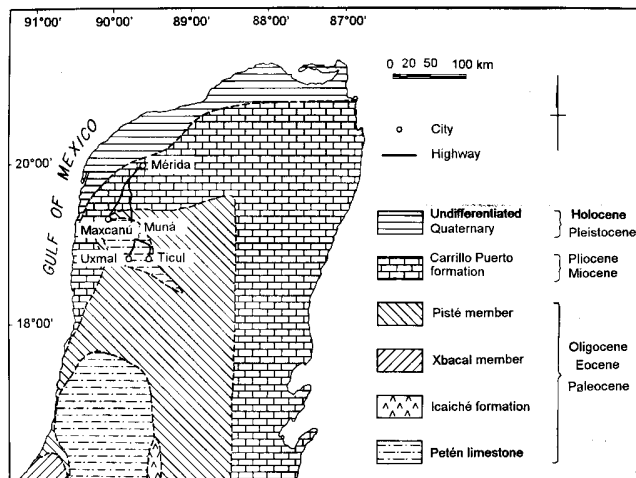


Figure 1. Geologic map of the Yucatán peninsula, taken from Bonet and Butterlin (1962), with data from West (1962). The studied samples were collected south of the Sierra de Ticul, in the vicinity of Maxcanú, Muná, Ticul, and Uxmal.

The peninsula is characterized by a thick sequence of evaporites that, in the northwest coastal plain, rest on Paleozoic andesite. In the northern platform and in the eastern block and Belize the evaporites rest on quartz and chlorite schist (Figure 2). In the northern platform, the schist underlies at a depth of 2,140 m the sediments of the Triassic-Jurassic Todos Santos Formation, which consist of red beds with intercalations of limolite, fine-grained sandstone, and cryptocrystalline dolomitic limestone. They are overlain by the Cretaceous evaporitic sequence which is about 3,000 m thick, consisting of anhydrite intercalated with limestone, dolomitic limestone, bentonite, and pelitic tuff; the association of rudists, miliolids, and nerineas sustains an environment of deposition of shallow salty waters within reefs. In the northwest coastal plain, the Lower Cretaceous is represented by plastic marl with intercalations of limestone, dolomitic limestone, anhydrite, shale, pyroclastics of andesitic composition, and andesite. The Paleocene-lower Eocene Icaiché formation spreads over the Cretaceous sequence. It is a white to gray crystalline limestone abundant in algae *Amphiroa*, mollusks, and serpulides, with intercalations of marl, shale containing pyrite and calcite, and green bentonite indicative of shallow marine bentonitic facies. Overlying the Icaiché formation is the Pisté formation, which is, in the northern platform, a fine-grained white limestone and, in

the northern coastal plain, a white to gray partly recrystallized limestone with intercalations of plastic marl and pyrite-containing limestone. The upper fossiliferous limestones of the Chichén-Itzá formation are differentiated in three members: (1) the Xbacal member, an intercalation of yellow marl, green shale, and yellowish white to gray impure limestone abundant in *Operculinoides catenula*, *Dyscocyclina cristensis*, Rotaliidae genus *Dictyokathina*, and Miliolidae; (2) the Pisté member, a relatively thick yellowish to white massive limestone rich in algae (*Clypeina*), foraminiferae (Valvulinidae, *Coskolina*), and Miliolidae characteristic of the Caribbean Eocene; (3) the Chumbec member, a white massive limestone with the appearance of saccaroidal marble, normally less than 100 m thick, with *Operculinoides willcoxi*, *Lepidocyclina pustulosa*, and Miliolidae. In the northwest coastal plain, the lower Oligocene is represented by white to gray marl with intercalations of clay, cream to gray compact limestone, and white to pink calcarenite with *Eulepidina* sp., *Nummulitides* sp., and *Biloculina* sp. The upper Oligocene consists of white to cream coquinooid limestone and calcarenite with algae, Miliolidae, *Lepidocyclina* sp., and *Camerina* sp. The Miocene-Pliocene Carrillo Puerto formation is a white powdery limestone, often recrystallized, containing *Archaias* sp., *Amphistegina* sp., algae, and ostracodes, with intercalations of light brown plastic marl. To the upper Miocene is assigned the Bacalar Formation which crops to the south of Quintana Roo. It is a whitish chalk containing clay that changes into marl, known locally as *sashcab*, with gypsum in the lower levels. The fauna comprises Peneroplidae, *Amphistegina* sp., and mollusks that could be Pliocene (Álvarez, 1954). It is overlain by red to white limestones alternating with yellow marls and sandstone lenses. The Pleistocene comprises, in the northwest plain, a white oolitic limestone with solution cavities intercalated with marl, and the Holocene includes the ever-present superficial caliche that covers the largest part of the peninsula (López-Ramos, 1979).

The clays in the Yucatán peninsula have been differentiated in pedogenic, detrital, and primary, neoformed, or direct-crystallized clays (Isphording, 1984). The first group of clays is associated with early pedogenic soil development and includes poorly crystallized kaolinite, boehmite, and traces of talc and chlorite. Their origin has been attributed to the accumulation and alteration of siliceous impurities from the parent limestones. The formation of kaolinite was possibly associated with the reaction between smectite and carbonic acid, which released Mg^{+2} , Na^{+} , HCO_3^{-} , and silicic acid, closely dependent on the buffer HCO_3^{-}/H_2CO_3 ; under high rainfall or topographic relief kaolinite would form over smectite. Liberated aluminum hydroxides would react to kaolinite, thereby disappearing boehmite in the more mature soils. Under detrital clays are the smectitic clays associated with detrital quartz, magnetite, ilmenite, and lesser kaolinite, derived from volcanic detritus deposited in lakes and lagoons prior to the uplift of the northern peninsula. They occur in the eastern block fault basin, east of Campeche, and in the Escárcega-Chetumal highway in

				Northwest Coastal Plain		Northern Platform		Belice and Eastern Block		
Era	System	Series	Formation	Column	Lithology	Column	Lithology	Column	Lithology	
Cenozoic	Quaternary	Holocene			Caliche		Caliche		Caliche	
		Pleistocene			White oolitic limestone with solution cavities, marl					
	Tertiary	Pliocene				White plastic marl with intercalated clay and minor limestone <i>Robulus vaughani</i>		White plastic marl with intercalated clay and minor limestone. <i>Robulus vaughani</i>		
			Carrillo Puerto							
		Miocene								White chalky limestone to white marl sashcab, thin layers of gypsum. <i>Peneroplis proteus</i>
			Bacálar							
		Eocene				White to gray marl with intercalations of clay and gray limestone. <i>Gaudryina jacksonensis</i> , <i>Spiroplectamina ala</i>				
			Chichen-Itzá	Chumbe Member		White massive limestone, like saccharoidal marble. <i>Operculinoides wilcoxi</i> , <i>Lepidocyclina pustulosa</i> , <i>Miliolidae</i>				
			Pisté Member			White massive limestone. <i>Clypeina</i> , <i>Valvulinidae</i> , <i>Coscolina</i>				
			Xbacal Member			White to gray limestone, plastic marl, shale. <i>Operculinoides catenula</i> , <i>Discocyclina</i> , <i>Rotulidae</i> , <i>Miliolidae</i>				
	Paleocene				White to gray limestone partly recrystallized, intercalations of plastic marl and gray limestone with pyrite. <i>Vaginulinopsis</i> ssp., <i>Globigerina cretacea</i>		White crystalline fine-grained limestone		Limestone, dolostone with black chert. Miscellaneous sp.	
		Icaiché			White to gray compact limestone, intercalations of marl and shale with pyrite and calcite. <i>Bulimina callahani</i> , <i>Alkormorphina velascoensis</i>		White crystalline limestone with intercalations of green bentonite. Macrofossils		Endogenous white dolomitic silicified limestone. Miliolids	
Cretaceous	Upper			Green plastic marl, intercalated shale, white limestone, dolomitic limestone, anhydrite, tuff, andesitic glass. <i>Globotruncana calciformis</i> , <i>Gumbelina globocasinata</i>		Anhydrite, minor intercalations of crystalline calcite and dolomitic calcite, bentonite. <i>Valvulina</i> sp.		Limestone, dolomitic limestone, thin cover of sandstone. Rudists, <i>Discocyclina</i> sp., <i>Globotruncana</i> sp., <i>Rotalia</i> sp., <i>Valvulina</i> sp.		
	Lower			Plastic marl with intercalation of limestone, dolomitic limestone, shale, anhydrite, andesitic tuff and andesite		Anhydrite with intercalations of bentonite, pelitic tuff, dolomitic limestone. Rudists, miliolids, nerineas, <i>Nummoloculina</i> sp.				
Mesozoic	Jurassic						Red beds with intercalations of siltstone, fine-grained sandstone, and cryptocrystalline dolomitic limestone			
	Triassic		Todos Santos							
Paleozoic					Andesite		Schist		Schist	

Figure 2. Schematic stratigraphic columns of the Yucatán peninsula. The stratigraphy of the northwest coastal plain is from the Chicxulub 1 well and the stratigraphy of the northern platform is from the Yucatán 1 well. Data from López-Ramos (1979).

Quintana Roo. Their transformation into kaolinite was prevented by uplift and faulting that turned basins into saline lakes, and by short rainy and long dry seasons. The third group of primary or direct-crystallized clays are those containing chlorite, talc, palygorskite-sepiolite, and montmorillonite. Talc and chlorite are attributed to the hyperhalmyrolic response of terrigenous sediments and to the high-Mg activities of the hypersaline waters. They occur in carbonate rocks and soils of the northern platform, associated with dolomitic rocks, formed by direct crystallization from the diagenetic alteration of dolomite, by reaction of silicic acid and dolomite, or of silicic acid, Mg^{+2} and HCO_3^- . Palygorskite-sepiolite crop out as isolated thin lenses or plug-like deposits within the limestones, formed by direct crystallization from marine waters or during diagenesis of dolomite (Bohor, 1975; Isphording, 1984). There is no significant ash to associate their origin to volcanic ash. Their formation, however, could be related with the alumina and silica carried in solution and deposited in

transitional marine environments, and which in alkaline pH form gels that precipitate as hydroxides, eventually transforming into high purity clays (Isphording, 1984).

SAMPLING AND ANALYTICAL METHODS

Palygorskite crops out in the Yucatán peninsula, within an area limited between 89° and 90°25' W and 18°25' to 18°70' N. The localities studied are in the vicinity of Maxcanú, Umán, Muná, Sacalum, and Ticul, near the Sierra de Ticul, easily reached from Mérida by Highways 66, 3, and 148 (Figure 1).

The rocks collected were plastic mudstone, limestone, and marl that required little preparation. They were crushed, dispersed ultrasonically in deionized water, and sedimented to separate coarser particles of carbonate, chert, opal, and gypsum from the clay. The clay was afterwards centrifuged to obtain the <2 μm fraction. The fine-grained carbonate intimately

associated with the clay was removed with 0.05 N acetic acid. Optical microscopy utilizing thin sections and oil-immersion methods was used to ascertain the mineralogy and textural relations of the rocks. The clay minerals were identified by X-ray diffraction (XRD) of oriented sedimented mounts of the centrifuged <2 μm fraction before and after solvation with ethylene glycol, using a D5000 diffractometer with filtered $\text{CuK}\alpha$ radiation and a goniometer speed of $0.5^\circ/2\theta/\text{min}$. Infrared absorption spectrometry (IR) was used to provide a more detailed characterization of the palygorskite structure and the associated H_2O , using a Perkin-Elmer 783 double beam IR spectrometer operated at a scanning speed of $1,000\text{ cm}^{-1}/\text{min}$ from $4,000\text{ cm}^{-1}$ to $2,000$ and at $500\text{ cm}^{-1}/\text{min}$ between $2,000\text{ cm}^{-1}$ and 200 wavenumbers. The specimens were pressed discs prepared from dry clay dispersed in KBr. Chemical analyses were done by wet chemistry for CO_2 , H_2O , and Na, and by X-ray fluorescence (XRF) for the remaining major elements. Morphology and microtextural relations were determined on unpolished flat specimens by scanning electron microscopy (SEM) in the secondary image mode. The composition of selected mineral phases in the samples was analyzed by energy dispersive spectrometry (EDS) coupled to the SEM. The analyses by this technique are considered semi-quantitative.

RESULTS

The studied area is around the Sierra de Ticul or Puuc. The sierra is the reef that dissects the Yucatán peninsula, separating the central lowland from the northern platform. It consists of a compact, dense, fossiliferous calcarenite that contains minor subhedral quartz, oolites; algae *Lithothamnium*, *Amphiroa*, and *Archacolithothamnium* species, and foraminifera *Homotema* and *Rosalina* species. Overlying the calcarenite is a diagenized magnesium limestone containing minor quartz and acicular calcite (Table 1). The lower contact of the calcarenite is with the limestone marl that extends around the sierra.

South of the sierra and 3 km N of Maxcanú, a white to yellowish plastic palygorskite-rich mudstone crops out. The outcrop is not less than 12 m high and 10 m wide. The mudstone is, on the northern side, in contact with a reddish hard compact limestone that, about 6 m from the contact with the palygorskite mudstone, changes to a gray hard compact partly recrystallized limestone (Table 1, Figure 3, a). On the southern side of the outcrop and under, the clay is in contact with white diagenized magnesium limestone of granoblastic texture, consisting of rhombohedral subhedral calcite (Table 1, Figure 3, b). This white limestone contains higher Mg, Si, and Al than the red limestone (Table 1). Bore-holes given around Maxcanú down to 1.5 m, showed palygorskite associated with calcite, gypsum, and chert nodules.

In the other localities around Umán, Muná, Chapab, Uxmal, and Ticul, palygorskite-rich mudstone occurs as lenses less than 3 m high, extending over 15 m in diameter. The

Table 1. Chemical composition of limestones [wt%].

	Composition					
	Limestones			Chalks ³		
	Dolomitic ¹	Red ²	White ³	Calcareous	Mg calcareous	Dolomitic
CaO	46.19	52.90	50.64	53.35	50.50	30.90
MgO	5.70	0.21	1.01	0.70	2.00	19.73
Na ₂ O	na	0.32	0.35	na	0.40	na
SiO ₂	na	1.30	3.12	na	1.41	na
Al ₂ O ₃	na	0.41	1.13	na	1.39	na
Fe ₂ O ₃	na	0.57	0.29	na	1.47	na
CO ₂	41.49	41.85	45.57	43.12	41.86	45.93
Total	98.03	97.56	97.46	97.17	99.15	96.56

Note: ¹Dolomitic limestone overlying calcarenite at the Sierra de Ticul; ²Limestones from Maxcanú. ³Calcareous, Mg-calcareous, and dolomitic chalks from Ticul-Muná. na: not analyzed.

mudstone is overlain by dolomitic marl and caliche (Table 1). The lower contact is masked with calcareous marl (Table 1). The mudstone is light brownish green, dull, resinous, moist, soft, plastic, containing essentially pure palygorskite. Palygorskite additionally occurs associated with calcite and dolomite in the yellowish calcareous or dolomitic marl locally known as *sashcab*.

XRD and SEM studies on material collected at the contact between the mudstone and the white diagenized limestone in Maxcanú, indicate that palygorskite is associated with opal and well-formed tabular authigenic calcite that forms stalactitic growths (Figure 4). Abundant crystallization of palygorskite occurs on the surface of rhombohedral subhedral calcite (Figure 4, d). The morphology, crystal habit, and composition of the authigenic calcite are significantly different from the subhedral rhombohedral and acicular calcite that characterized the white diagenized limestone (Figures 3 and 5). In the same material, further from the mudstone-limestone contact, occur irregular undulated lamellar crystals of high potassium content that appear to correspond to interstratified illite/montmorillonite (Figure 6). They do not show any superficial alteration that would suggest transformation to palygorskite. They are distinct from other irregular lamellar crystals that do not contain potassium, but do show superficial alteration to feathery palygorskite (Figure 6).

In Yaxcabá, Akil, Ticul, Hacienda de Yok'at in Ticul, and in Uayma, a mudstone, locally known as *kat*, crops out, which contains disordered kaolinite associated with minor calcite and quartz.

MINERALOGY

Palygorskite is the dominant clay mineral in the mudstone, where it appears as bundles of fine feathery crystals, associated with illite/smectite, smectite, possible illite and chlorite, and authigenic calcite (Figure 7). It is monoclinic, characterized by its reflections $\bar{1}21$ and 121 (Christ *et al.*,

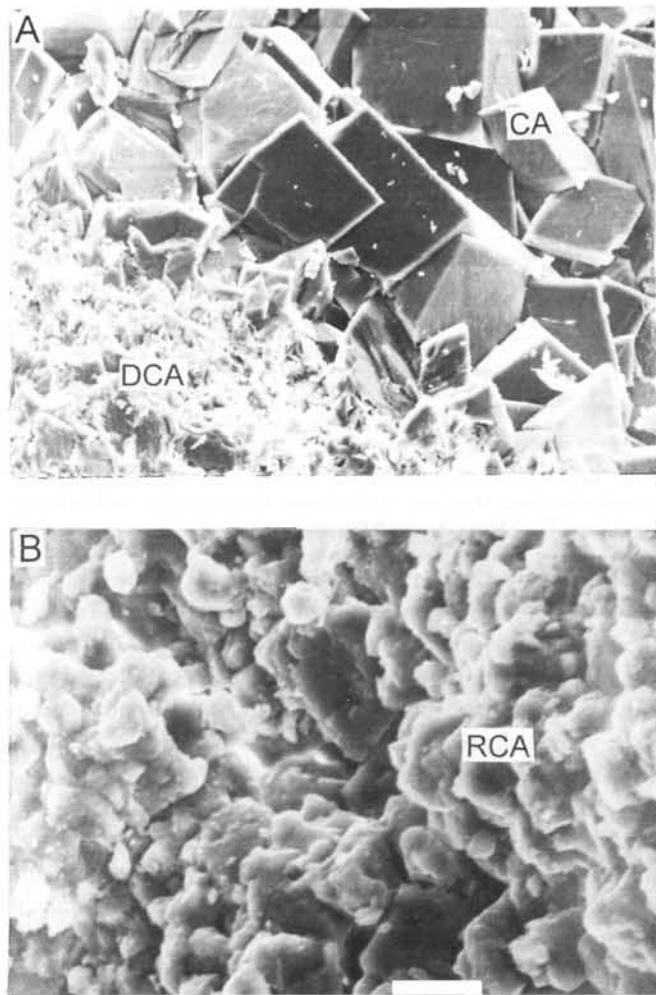


Figure 3. SEM micrograph of the limestones: A, red limestone 6 m from the contact with the palygorskite-rich mudstone, showing well-crystallized calcite (CA); B, white diagenized limestone underlying the palygorskite-rich mudstone, showing subhedral rhombohedral calcite (RCA). Horizontal bar represents 1 micrometer. Maxcanú.

1969) (Table 2). The chemical composition (Table 3) corresponds to the formula:



calculated for a 21-oxygen cell (Drits and Sokolova, 1971). $^{\text{IV}}\text{Al}$ is within the limits of 0.01 and 0.69 (Weaver and Pollard, 1975) or 0.12 and 0.66 (Newman and Brown, 1987). Octahedral cations add to 3.99, between the limits of 3.76 and 4.44 set for dioctahedral structures (Newman and Brown, 1987). It is within the range of composition of palygorskite from various localities (Table 4). The composition calculated for the octahedral layer (Figure 8) is similar to palygorskite from other locations (Chahi *et al.*, 1993). IR analysis indicates OH-stretching at 3520 and 3590 cm^{-1} slightly displaced from the wavenumbers reported for palygorskite (Serna and Vanscoyoc, 1978); H_2O bending at 1,640 cm^{-1} , Si-O stretching at 1,025 and bending at 480 cm^{-1} , and other vibrations at 1185, 1120, 1090, and 980 cm^{-1} and at 520 and 440 cm^{-1} , which confirm tetrahedral and octahedral substitutions.

SEM data show feathery palygorskite on smectite flakes (Figure 6) and on rhombohedral calcite from the diagenized limestone (Figure 4). Palygorskite associated with calcite, dolomite, and very minor quartz occurs in plastic calcareous marl around Ticul and Muná. When associated with calcite and minor quartz, reflection $d_{040} = 4.54 - 4.49\text{\AA}$ is much more intense than $d_{011} = 10.52\text{\AA}$. When associated with calcite and dolomite and minor quartz, reflection d_{011} always is more intense than d_{040} .

Interstratified illite/smectite occurs as a minor component, characterized by weak XRD peaks at 12.52 \AA and 4.907 \AA that suggest a 1:1 interstratification. Other expected reflections (as d_{004} at 6.35 \AA or d_{006} at 4.23 \AA) are masked by those of palygorskite. The mineral has a foliate lamellar texture (Figure 6), irregular undulated shape and edges, size less than 2 μm . Palygorskite is not formed on its surface. The structural formula calculated for a 22-oxygen cell from the semi-quantitative composition (Table 5) determined by EDS is:



The ratio of tetrahedral to octahedral charges 31.94/11.17 and the sum of octahedral cations corresponds to a dioctahedral mineral, with the smectite component possibly being of the beidellite type. The tetrahedral charge of 0.03, octahedral of 11.17, and layer charge of 0.44 for the half-cell calculated from the structural formula are between the domains of illites and smectites, or within the area of the I/Sm interstratified (Figure 9, with data from Yoder and Eugster, 1955; Weaver and Pollard, 1975; Köster, 1982; Srodon and Eberl, 1984; Chahi *et al.*, 1993).

Disordered kaolinite over 90% pure, associated with minor calcite and quartz, never with palygorskite, occurs in mudstone. It is of fine particle size, plastic. By XRD is characterized by a 001 peak broad and symmetrical, and 02 $\bar{1}$, 20 $\bar{1}$, and 13 $\bar{1}$ peaks (Table 6) asymmetrical towards smaller d spaces. Smectite is characterized by an intense broad reflection extending from 14.75 to 15.44 \AA that is displaced to 17.5 \AA when solvated. Other possible reflections are masked by those of palygorskite. Illite could only be identified by a low-intensity 10 $\bar{1}$ reflection in some samples that did not contain palygorskite, which has its 110 reflection at this same position. A second peak at 4.91 \AA coincides with the interstratified illite/smectite. It has been reported to be a 1Md-illite (Schultz, 1971). Calcite occurs, authigenic, as well-formed tabular crystals that form stalactitic growths at the contact of the clay with the white limestone. Its composition and morphology are different from the euhedral rhombohedral calcite in the white limestone, suggesting a different origin. Minor amounts of acicular calcite occur in the white limestone and calcareous chalk (Figure 7). Opal-A forms globular aggregates associated with palygorskite in the mudstones and at the clay-white limestone contact (Figure 4). Chert nodules, light brown, up to 6 in diameter, occur in the calcareous shale. Gypsum occurs in

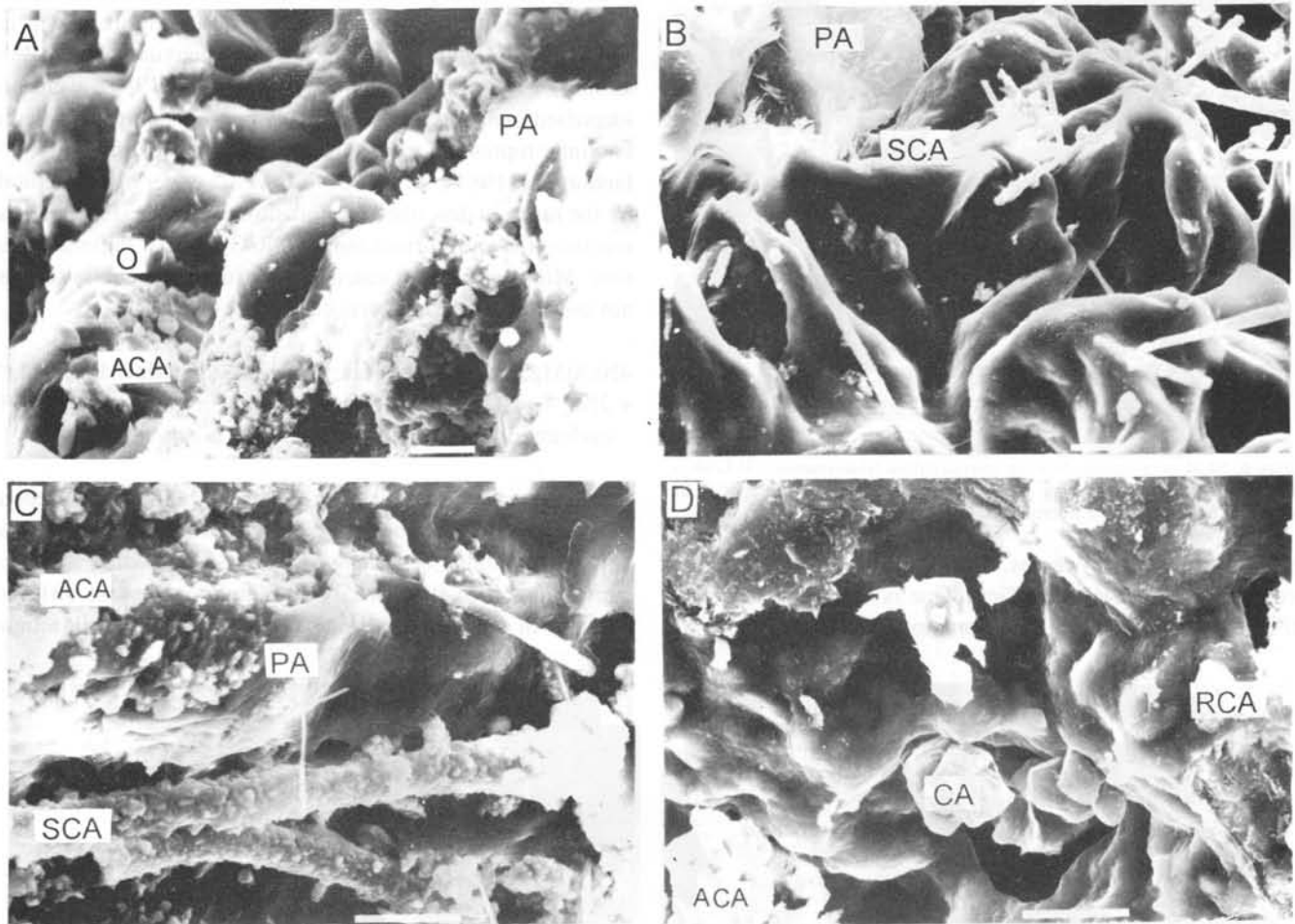


Figure 4. SEM micrographs of the white limestone in contact with the palygorskite-rich mudstone, showing: A, authigenic tabular calcite (ACA), opal (O), palygorskite (PA); B, stalactitic growths of authigenic calcite (SCA); C, stalactites of authigenic calcite (SCA), authigenic calcite (ACA), and palygorskite (PA); D, rhombohedral calcite (RCA), authigenic calcite (ACA), and calcite (CA). Horizontal bar represents 1 micrometer. Maxcanú.

bundles of three in long fibres of satin spar and nodules in the calcareous shale.

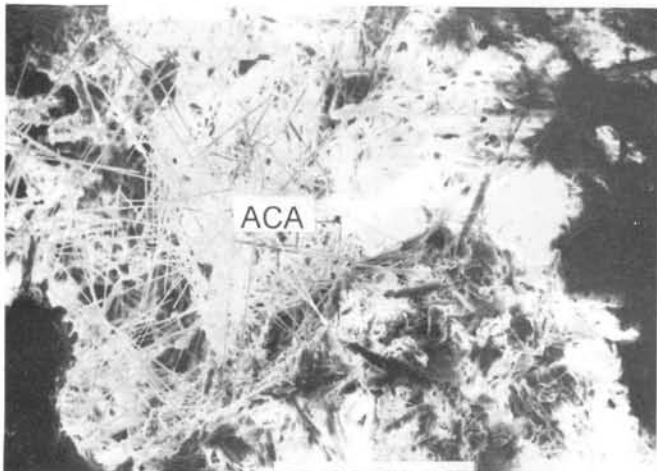


Figure 5. SEM micrograph of acicular calcite (ACA), sampled at the contact between palygorskite-rich mud and white limestone. Horizontal bar is 1 micrometer. Maxcanú.

DISCUSSION

The data available on the geology and stratigraphy of the Yucatán peninsula are far from complete, consequently influencing any attempt to establish the genesis of palygorskite. The palygorskite-rich mudstone deposits that occur around the Sierra de Ticul, are in undifferentiated Eocene-Oligocene terrain (Bonet and Butterlin, 1962; Bohor, 1975). At Maxcanú, the mudstone is in contact with the red and gray hard compact partly recrystallized limestone of the Pisté formation, which defines the lower limit of palygorskite formation. Overlying the mudstone, is the white diagenized limestone of higher contents of Mg, Si, and Al of the Pisté or Chumbec members of the upper Eocene Chichén-Itzá formation. Lenses of essentially pure palygorskite occur in Oligocene calcareous marl, overlain by dolomitic marl.

The morphology of palygorskite suggests tranquil crystallization rather than deposition of suspended or transported detrital material. The absence of clastic minerals, turbidites, or ripple marks sustains that the clay was not transported and was

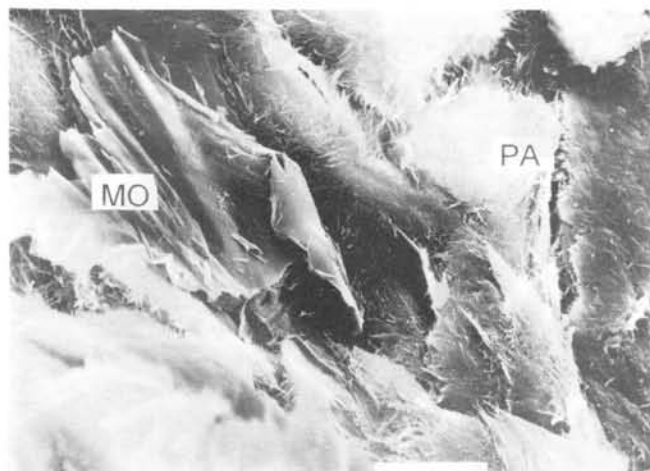
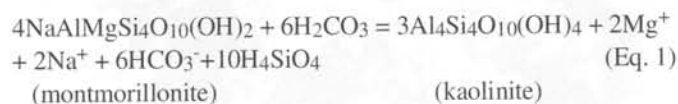


Figure 6. SEM micrograph showing interstratified illite/smectite (ILL/MO), montmorillonite (MO) altering into palygorskite, and palygorskite (PA). Horizontal bar represents 1 micrometer. Maxcanú.

formed by *in situ* processes. Two distinct clay associations occur around the Sierra de Ticul. One is represented by over 90% pure disordered kaolinite, common in the mudstone or *kat*

used by the local potters, associated with minor calcite and quartz. Interstratified kaolinite/montmorillonite (Schultz, 1971), detrital anatase (Schultz, *op. cit.*), dehydrated halloysite (Bohor, 1975), talc or chlorite (Ispording, 1984), were not identified in the present study. This fine-crystallite disordered kaolinite represents mature pedogenic soils (Quiñones, 1975; Ispording, 1984), formed from smectite under higher rainfall by the reaction described by Equation 1 (Berner, 1971). In the reaction, the equilibrium buffer $\text{H}_2\text{CO}_3/\text{HCO}_3^-$ defines direction. Minor associated calcite is detrital. This kaolinite does not associate with palygorskite.



Andesitic glass occurs with anhydrite in the Cretaceous evaporitic sequence, but neither andesitic glass or anhydrite appear in younger sediments. The shale, bentonite, and gypsum common to the Tertiary formations represent different volcanic or sedimentary events. Gypsum, found in soils around

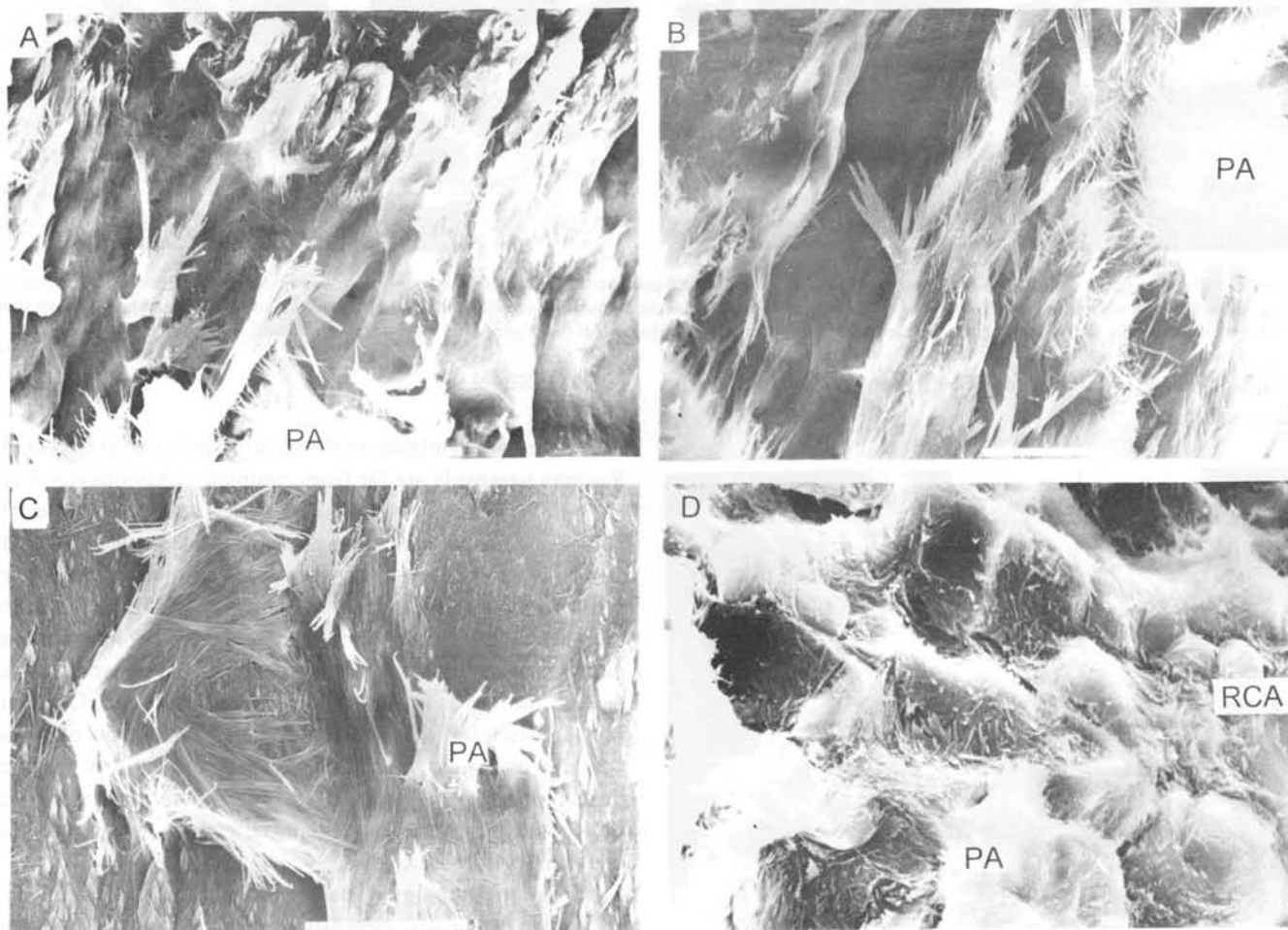


Figure 7. A–D. SEM micrographs of palygorskite (PA). In D, palygorskite growths on rhombohedral calcite (RCA) from the diagenized white limestone. Horizontal bar represents 1 micrometer. Maxcanú.

Table 2. X-ray diffraction data for palygorskite.

hkl	Sapillo ¹		Yucatán	
	d (Å)	I/I ₀	d (Å)	I/I ₀
011	10.44	100	10.36	100
002	6.36	13	6.36	10
031	5.39	9	5.34	9
040	4.466	20	4.441	24
121	4.262	22	4.247	11
013, 121	4.129	2	4.131	11
122	3.679	15	3.656	7
132	3.348	7	3.366	8
004	3.179	12	3.180	13
123	3.096	16	3.124	10
160, 044	2.589	10	2.590	10
211, 161	2.539	20	2.544	13

¹ Data from Christ and coworkers (1969).

Maxcanú, indicates crystallization from less saline and colder environments than those prevailing in the Cretaceous. Palygorskite in the Tertiary had to form from smectite, dolomite, or by direct precipitation. An origin that would associate palygorskite with air-borne volcanic detritus would not appear so convincing, given the high purity of the mineral and the absence of detrital components.

Table 3. Chemical composition of palygorskite from Yucatán.

Composition	
[wt%]	
SiO ₂	53.75
Al ₂ O ₃	11.56
Fe ₂ O ₃	1.78
FeO	0.34
TiO ₂	0.31
MgO	10.41
CaO	0.98
Na ₂ O	0.63
K ₂ O	0.62
H ₂ O ⁺	8.72
H ₂ O ⁻	10.69
[mole]	
Si	7.61
^{IV} Al	0.39
^{VI} Al	1.54
Mg	2.19
Fe ⁺³	0.19
Fe ⁺²	0.04
Ti	0.03
Ca	0.15
Na	0.17
K	0.11
O	21

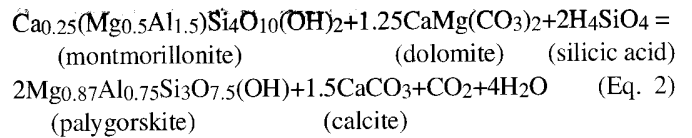
Table 4. Composition of palygorskites from various localities¹.

Locality	Si	^{IV} Al	^{VI} Al	Fe ⁺³	Mg	Fe ⁺²	Ti	Ca	Na	K
Georgia	7.79	0.21	1.57	0.38	1.88			0.32	0.09	0.04
USA	7.81	0.19	1.66	0.36	1.83			0.01	0.45	0
Japan	7.82	0.18	1.57	0.24	2.04			0.36	0	0
Yucatán	8.00	0	1.53	0.42	2.12			0.03	0.01	0.09
Yucatán ²	7.61	0.39	1.54	0.19	2.19	0.04	0.03	0.15	0.11	0.17

¹Data from Chahi and coworkers (1993).

²Present work.

A second clay association is represented by palygorskite. Experimental SEM evidence (Figure 6) seems to indicate that, in Maxcanú, montmorillonite was transformed to palygorskite. At the contact between the palygorskite-rich mudstone and the white diagenized limestone, in addition to palygorskite, authigenic calcite and opal (Figure 4) occur. Such association fits the reaction between montmorillonite, dolomite, and siliceous acid to palygorskite and calcite, described to occur in shallow coastal peri-marine environments (Weaver and Beck, 1977) (Equation 2). Excess SiO₂ would form opal.



Direct precipitation of palygorskite has been indicated as a possible genetic mechanism (Ispording, 1984). The reaction would be between soluble alumina and silica carried into the coastal basins, where prevalent marine alkaline environment would assure precipitation of palygorskite and sepiolite. However, the small size and sparing distribution of the deposits found in Yucatán do not sustain a massive precipitation. In the present study, talc, chlorite, and sepiolite were not identified

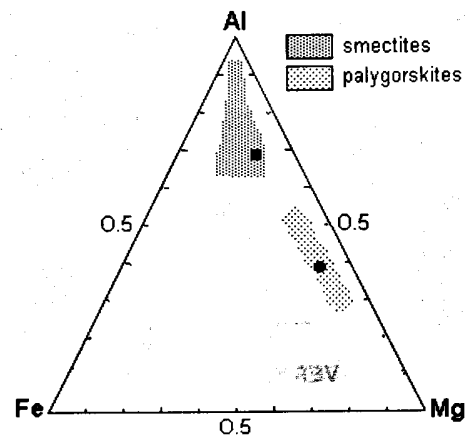


Figure 8. Composition of the octahedral sheets of palygorskite and interstratified illite/smectite. Black dots represent minerals from Maxcanú, Yucatán.

Table 5. Chemical composition of interstratified illite/smectite.

Composition	
[wt%]	
SiO ₂	50.65
Al ₂ O ₃	15.24
Fe ₂ O ₃	3.24
TiO ₂	0.19
MgO	3.66
CaO	0.85
Na ₂ O	0.42
K ₂ O	2.33
[mole]	
Si	7.94
IV Al	0.06
VI Al	2.75
Mg	0.85
Fe ⁺³	0.38
Ti	0.02
Ca	0.14
Na	0.13
K	0.47
O	22

and palygorskite occurs instead associated with calcite and dolomite. The intensities of the palygorskite X-ray reflections change depending on whether the mineral is associated with calcite or with calcite plus dolomite, suggesting that the abundance of either Ca or Ca+Mg affects crystallization. The association of palygorskite with carbonates could imply that: (1) calcite and dolomite are detrital, and palygorskite either precipitated from the reaction between acid solutions carrying soluble silica and alumina and stagnant marine alkaline waters, or simpler hydroxides, talc, or chlorite formed and later transformed into palygorskite; (2) calcite and dolomite are authigenic, or calcite is as experimental data prove, and reac-

Table 6. X-ray diffraction data for disordered kaolinite from Ticul, Yucatán.

hkl	d (Å)	I / I ₀
001	7.49	21
021	4.52	100
002	3.573	47
201	2.568	58
131	2.526	68
003	2.390	31
220	2.194	13
203	2.100	5
204	1.684	13
133	1.641	26
060	1.495	13

tion between precursor montmorillonite, dolomite, and solutions carrying soluble silica formed palygorskite; (3) the palygorskite-rich mudstone lenses overlain by dolomitic marl and underlain by calcareous marl relatively low in Mg, Si, and Al, resulted from silica and alumina solutions reacting with precursor limestone or calcareous marl. Gypsum and chert nodules that occur associated with palygorskite indicate a not so saline environment of deposition where excess H₄SiO₄ was available to form chert; this silicic acid either came from precursor limestone or dolomitic limestone, as experimental data indicate, came from elsewhere, or both. Crystallization of palygorskite is intense on rhombohedral calcite from the white diagenized limestone; this calcite possibly contained sufficient Mg to react with Si-rich solutions to palygorskite.

In conclusion, experimental data supports a diagenetic model for the origin of palygorskite, where precursor montmorillonite reacted with dolomitic limestone and silicic acid, with separation of calcite. The proportion of opal relative to clay is sufficiently high to presume that some of the required silicic acid could come from other sources distinct from the limestones. The environment was back-reef lagoon marine Mg-rich, more saline than the normal sea water, and of higher temperature. Other possible genetic mechanisms do not seem so feasible in Yucatán. Reaction of detrital smectite and illite with Mg to palygorskite with evaporation of silicic acid (Sánchez and Galán, 1995) is not supported in this case, by the lack of alteration of interstratified illite/smectite into palygorskite. An origin similar to that reported for the Florida palygorskite (Bohor, 1975), based on the past-time association of the Florida and Yucatán peninsulas, has been strongly argued against (Isphording, 1984) from mineralogical and geological reasons.

ACKNOWLEDGMENTS

The author is indebted to P. Altúzar, M.L. Chávez, A. Lozano, and M. Reyes for their analytical work. A. Altamira and A. Maturano assisted with photographic and laboratory work.

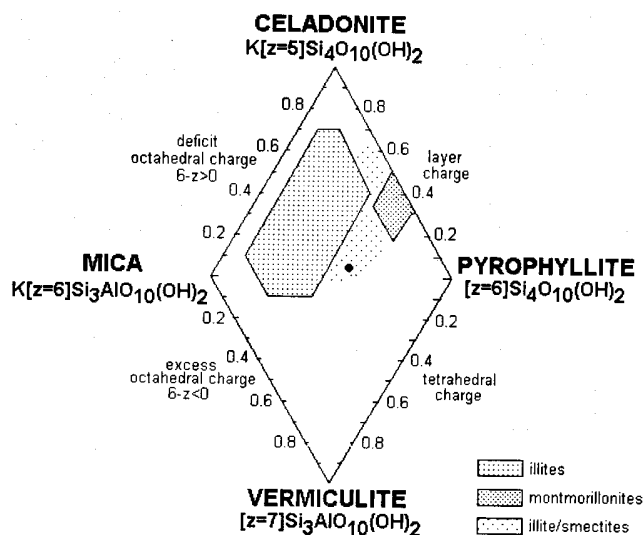


Figure 9. Charge distribution of the interstratified illite/smectite from Maxcanú and phyllosilicates, for half-cell (with data from Chahi *et al.*, 1993; Srodon and Eberl, 1984; Köster, 1982; Weaver and Pollard, 1975; Yoder and Eugster, 1955).

BIBLIOGRAPHICAL REFERENCES

- Álvarez, Manuel, Jr., 1954, Exploración geológica preliminar del Río Hondo, Quintana Roo: Boletín de la Asociación Mexicana de Geólogos Petroleros, v. 6, p. 207-213.
- Arnold, D., and Bohor, B.F., 1978, Attapulgite and Maya Blue—an ancient mine comes to light: *Archaeology*, v. 28, p. 23-29.
- Berner, R.A., 1971, Principles of chemical sedimentation: New York, McGraw-Hill, 191 p.
- Bohor, B.F., 1975, Attapulgite in Yucatán, in de Pablo-Galán, Liberto, ed., International Clay Conference Field Trip: Universidad Nacional Autónoma de México, Instituto de Geología, México, D.F., Guidebook FT-4, p. 95-125.
- Bonet, Federico, and Butterlin, Jacques, 1962, Stratigraphy of the northern part of the Yucatán Peninsula, in Murray, G.E., and Weidie, E., eds., Guidebook Yucatán Peninsula Field Trip: New Orleans Geological Society, New Orleans, Guidebook, p. 52-57.
- Butterlin, Jacques, and Bonet, Federico, 1960, Microfauna del Eoceno inferior de la Península de Yucatán: Universidad Nacional Autónoma de México, Instituto de Geología, Paleontología Mexicana 2, 18 p.
- Callen, R.A., 1984, Clays of the palygorskite-sepiolite group—depositional environment, age, and distribution, in Singer, Urieh, and Galán, Emilio, eds., Palygorskite-sepiolite occurrences, genesis, and uses: *Developments in Sedimentology*, v. 37, p. 1-37.
- Chahi, Azzedine; Duplay, Joelle, and Lucas, Jacques, 1993, Analyses of palygorskites and associated clays from the Jbel Rhassoul (Morocco)—chemical characteristics and origin of formation: *Clays and Clay Minerals*, v. 41, p. 401-411.
- Christ, C.L.; Hathaway, J.C.; Hostetler, P.B.; and Shepard, A.O., 1969, Palygorskite—new X-ray data: *American Mineralogist*, v. 54, p. 198-205.
- Drits, V.A., and Sokolova, G.V., 1971, Structure of palygorskite: *Soviet Physics Crystallography*, v. 16, p. 183-185.
- Estéoule-Choux, Janine, 1984, Palygorskite in the Tertiary deposits of the Armorican Massif, in Singer, Arieh, and Galán, Emilio, Palygorskite-sepiolite occurrences, genesis, and uses: *Developments in Sedimentology*, v. 37, p. 59-73.
- Galán, Emilio, and Castillo, Antonio, 1984, Sepiolite-palygorskite in Spanish Tertiary basins—genetical patterns in continental environments, in Singer, Arieh, and Galán, Emilio, Palygorskite-sepiolite occurrences, genesis, and uses: *Developments in Sedimentology*, v. 37, p. 87-124.
- Isphording, W.C., 1973, Discussion of the occurrence and origin of sedimentary palygorskite-sepiolite deposits: *Clays and Clay Minerals*, v. 21, p. 591-401.
- 1984, The clays from Yucatán, Mexico; a contrast in genesis, in Singer, Arieh, and Galán, Emilio, eds., Palygorskite-sepiolite occurrences, genesis, and uses: *Developments in Sedimentology*, v. 37, p. 75-86.
- Jones, B.F., 1986, Clay mineral diagenesis in lacustrine sediments: *U.S. Geological Survey Bulletin*, v. 1578, p. 291-300.
- Jones, B.F., and Galán, Emilio, 1988, Sepiolite and palygorskite, in Bailey, S.W., ed., *Hydrous Phyllosilicates: Reviews in Mineralogy*, v. 19, Washington, D.C., Mineralogical Society of America, p. 631-674.
- Köster, H.M., 1982, Layer silicates, pt. 1, in van Olphen, H., and Veniale, E., The crystal structure. *Proceedings International Clay Conference Bologna-Pavia 1981*: Amsterdam, Elsevier, p. 41-71.
- López-Ramos, Ernesto, 1979, *Geología de México*: México, D.F., t. 3, 445 p., edición escolar.
- Newman, A.C.D., and Brown, G., 1987, The chemical constitution of clays, in Newman, A.C.D., ed., *Chemistry of clays and clay minerals*: London, Mineralogical Society, Monograph, v. 6, p. 1-128.
- Pablo-Galán, Liberto de, 1971, Attapulgita de Ticul, Yucatán: Universidad Nacional Autónoma de México, Instituto de Geología, Boletín, v. 92, 53 p.
- Patterson, S.H., 1974, Fuller's earth and other industrial mineral resources of the Meigs-Attapulgis-Quincy District, Georgia and Florida: U.S. Geological Survey Professional Paper, v. 628, 45 p.
- Quiñones, H., 1975, Soil study area 4; Intrazonal soils of northern Yucatán Peninsula, in de Pablo-Galán, Liberto, ed., International Clay Conference, Field Trip Guidebook FT-4: Universidad Nacional Autónoma de México, Instituto de Geología, México, D.F., Guidebook FT-4, p. 70-93.
- Sánchez, Carlos, and Galán, Emilio, 1995, An approach to the genesis of palygorskite in a Neogene-Quaternary continental basin using principal factor analysis: *Clay and Clay Minerals*, v. 30, p. 225-238.
- Schultz, L.G.; Shepard, A.O.; Blackman, P.D., and Starkey, H.C., 1971, Mixed layer kaolinite-montmorillonite from the Yucatán Peninsula, Mexico: *Clays and Clay Minerals*, v. 19, p. 137-150.
- Serna, C.J., and Vanscoyoc, G.E., 1978, Infrared study of sepiolite and palygorskite surfaces, in Mortland, M.M., and Farmer, V.C., eds., International Clay Conference: Amsterdam, Elsevier, International Clay Conference, Proceedings, p. 197-206.
- Shadfan, H.; Mashhady, A.S.; Dixon, J.B.; and Hussen, A.A., 1985, Palygorskite from Tertiary formations of eastern Saudi Arabia: *Clays and Clay Minerals*, v. 33, p. 451-457.
- Singer, Arieh, 1979, Palygorskite in sediments; detrital, diagenetic, or neofomed—a critical review: *Geologische Rundschau*, v. 68, p. 996-1008.
- 1984, Pedogenic palygorskite in the arid environment, in Singer, Arieh, and Galán, Emilio, eds., Palygorskite-sepiolite occurrences, genesis, and uses: *Developments in Sedimentology*, v. 37, p. 169-177.
- Singer, Arieh, and Norrish, Keith, 1974, Pedogenic palygorskite occurrences in Australia: *American Mineralogist*, v. 59, p. 508-517.
- Srodon, Jan, and Eberl, D.D., 1984, Illites, in Bailey, S.W., ed., *Micas*: Washington, D.C., Mineralogical Society of America, Reviews in Mineralogy, v. 13, p. 495-539.
- Tardy, Yves, and Garrels, R.M., 1974, A method of estimating the Gibbs energies of formation of layer silicates: *Geochimica et Cosmochimica Acta*, v. 38, p. 1101-1116.
- Van den Heuvel, R.C., 1966, The occurrence of sepiolite and attapulgitite in the calcareous zone of a soil near Las Cruces, New Mexico: *Clays and Clay Minerals*, National Conference, 13, Proceedings, p. 193-208.
- Weaver, C.E., and Pollard, L., 1975, The chemistry of clay minerals: Amsterdam, Elsevier, *Developments in Sedimentology*, v. 15, 213 p.
- Weaver, C.E., and Beck, K.C., 1977, Miocene in the SE United States—A model for chemical sedimentation in a peri-marine environment: *Sedimentary Geology*, v. 17, p. 1-234.
- Weidie, A.E., Jr., and Murray, G.E., 1962, Geologic log road Mérida to Campeche, in Murray, G.E., and Weidie, E., eds., Guidebook Yucatán Peninsula Field Trip: New Orleans Geological Society, New Orleans, Guidebook, p. vii-xv.
- West, R.C., 1962, Physical geography of the Yucatán Platform, in Murray, G.E., and Weidie, E., eds., Guidebook Yucatán Peninsula Field Trip: New Orleans Geological Society, New Orleans, Guidebook, p. 58-63.
- Yaalon, D.H., and Wieder, M., 1976, Pedogenic palygorskite in some arid brown (calciorthid) soils of Israel: *Clays and Clay Minerals*, v. 11, p. 73-80.
- Yoder, H.S., Jr., and Eugster, H.P., 1955, Synthetic and natural muscovites: *Geochimica et Cosmochimica Acta*, v. 8, p. 225-280.

Manuscript received: December 15, 1995.

Corrected manuscript received: June 12, 1996

Manuscript accepted: June 28, 1996.